HHS Public Access

Author manuscript

J Immunol. Author manuscript; available in PMC 2016 June 01.

Published in final edited form as:

J Immunol. 2015 June 1; 194(11): 5465–5471. doi:10.4049/jimmunol.1403249.

Lung is protected from spontaneous inflammation by autophagy in myeloid cells

Masashi Kanayama[*], **You-Wen He**[*], and **Mari L. Shinohara**[*,§]

[*]Department of Immunology, Duke University Medical Center, Durham, NC 27710, U.S.A.

[§]Department of Molecular Genetics and Microbiology, Duke University Medical Center, Durham, NC 27710, USA

Abstract

Lung is constantly exposed to outer environment; thus, the lung must maintain a state of immune ignorance or tolerance not to over-respond to harmless environmental stimuli. How cells in the lung control immune responses under the environmental exposure is not fully understood. Here, we found that autophagy plays a critical role in the lung-specific immune regulation to prevent spontaneous inflammation. Autophagy in pulmonary myeloid cells plays a role not only in maintaining low burdens of environmental microbes in the lung, but also in lowering mitochondrial reactive oxygen species production and raising a threshold in responding to Toll-like receptor 4 (TLR4) ligands in alveolar macrophages. Based on the mechanisms, we also found that intranasal instillation of antibiotics or an inhibitor of reactive oxygen species was efficient to prevent spontaneous pulmonary inflammation. Thus, autophagy in myeloid cells, particularly in alveolar macrophages, is critical in inhibiting spontaneous pulmonary inflammation; but pulmonary inflammation caused by dysfunctional autophagy is pharmacologically prevented.

Introduction

The lung is constantly exposed to environmental oxygen, air dusts and microbes. Therefore, to avoid inflammatory responses to harmless and ambient levels of stimulations, the lung developed site-specific immune regulatory strategies to restrain inflammation, imparted by unique resident cellular populations. Alveolar macrophages (AMs) are lung-resident macrophages. In terms of inflammation in the lung, AMs have two opposite functions (1). AMs inhibit inflammation in the lung, and are equipped with inhibitory factors to terminate the ongoing inflammation by upregulating anti-inflammatory receptors, such as CD200R, TREM2 and MARCO, on the cell surface. AMs are also known as an inducer of regulatory T cells (Tregs) by supplying TGF-β and retinoic acid (2). On the other hand, AMs are activated by PRR-mediated signaling and produce proinflammatory cytokines and chemokines as immune sentinels in the lung (1). Phagocytic function of AMs also contributes to clear viral, bacterial and fungal pathogens (3). Pro-inflammatory immune

Address correspondence and requests to Dr. Mari L. Shinohara, Department of Immunology, DUMC3010, Duke University Medical Center, Durham, NC 27710. mari.shinohara@duke.edu.

Disclosures

The authors have no financial conflict of interest.

responses by AMs result in the recruitment of other immune cell types, such as neutrophils and inflammatory monocytes; therefore, AMs have to fine-tune the threshold, above which an infection is perceived as a threat, in detecting ligands of pattern recognition receptors (PRRs) and in exerting immune responses.

Autophagy is a cellular process which degrades unwanted cytoplasmic components such as old proteins, organelles and intracellular pathogens. Autophagy is induced by signaling through PRRs and cytokine receptors to eliminate intracellular microbes through autophagosomal digestion (4–11). Recent studies showed that autophagy regulates immune responses in pathological conditions. For example, autophagy removes reactive oxygen species (ROS)-generating mitochondria and suppresses inflammasome-mediated IL-1β/IL-18 production (12) to downregulate pro-inflammatory responses. In viral and bacterial infections, autophagy mediates antigen processing and presentation to enhance adoptive immune responses (13, 14). In fungal infection, we have recently reported that autophagy enhances NFκB-mediated chemokine production in tissue-resident F4/80^{hi} macrophages by sequestering an NFκB inhibitor, A20 (15). In particular, autophagy in pulmonary myeloid cells, including AMs, is known to prevent excessive immune responses and inflammation under pathological conditions such as endotoxemia, cystic fibrosis and hemorrhagic shock (16–19). However, the impact of autophagy on the maintenance of immune homeostasis under non-pathological condition remains unclear.

In this study, we showed that mice lacking *Atg7* in myeloid cells spontaneously develop pulmonary inflammation. Without autophagy, the lung inflammation was initiated between 2 and 3-wks old of age and largely mediated by infiltration of innate immune cells such as neutrophil, Ly6C^{+} monocytes and DCs. Interestingly, the conditional *Atg7* knock-out mice did not induce inflammation in organs other than the lung. Autophagy in myeloid cells plays a role in maintaining a state of immune ignorance or tolerance to harmless stimuli in the lung by 1) lowering bacterial/fungal loads in the lung, 2) decreasing mitochondrial ROS (mtROS) production, and 3) increasing the detection threshold of PRR ligands to perceive as a threat. Indeed, administration of antibiotics and treatment with an ROS inhibitor prevented the initiation of pulmonary inflammation in *Atg7* conditional knock-out (CKO) mice. Thus, autophagy inhibits spontaneous inflammation in the lung through controlling loads of environmental microbes and the sensitivity of AMs even in non-pathological condition.

Materials and Methods

Animals and Reagents

All the mice used here have the C57BL/6 background. *Atg7*$^{fl/fl}$ mice were described previously (20). *LysM*$^{cre/cre}$ mice were purchased from Jackson Laboratories. All the experiments were performed as approved by IACUC. Antibodies against CD45, CD11b, F4/80, TLR4, TLR2, CD4, CD3, CD11c, Siglec F, CD200R, Ly6G and Ly6C were purchased from BioLegend. Dectin-1 and dectin-2 antibodies were from AbD Serotec. Antibodies against TREM2 and MARCO were purchased by R&D. MitoSOX and Dihydroethidium (DHE) were purchased from Life Technologies. An ROS inhibitor, N-acetyl-L-cyteine (NAC) was purchased from Sigma.

Cell culture condition

AMs were FACS-sorted with MoFlo Legacy (Beckman Coulter) as $CD45^{+}CD11c^{hi}F4/80^{+}Siglec\text{-}F^{+}$, and cultured in the RPMI-1640 medium containing 10% FCS, penicillium/streptomycin (Sigma) and 2 mM of L-glutamine. For some experiments, AMs were stimulated with or without LPS (0–10 ng/ml) and/or N-acetylcysteine (NAC; 10mM) for 24 hrs.

Flow cytometry analysis

Lung tissues were minced and treated with collagenase D (1 mg/ml) at 37 °C for 30 min. Cells were then enriched by discontinuous density gradient centrifugation with Percoll (GE Healthcare), and numbers of total cells, staining with 0.4 % Trypan blue, were counted with a hemocytometer. Followed by cell staining with specific antibodies, cells were analyzed with FACS CantoTM II (BD) and the FlowJo software (Treestar inc) used for the acquisition and analysis of the data, respectively.

Evaluation of reactive oxygen species (ROS) production

AMs ($CD45^{+}CD11c^{hi}F4/80^{-}Siglec\text{-}F^{+}$) were incubated in the presence of DHE to detect general ROS levels (5 μM) or MitoSOX to detect mtROS levels (5 μM) for 30 and 10 min, respectively. After three-time of washing with warm HBSS, cells were fixed and the levels of ROS were determined by flow cytometory.

Histology

The lungs were obtained from 7 month old WT and *Atg7* CKO mice, fixed with Bouin's solution (Sigma), and embedded in paraffin. Sections were cut with 5 μm thickness and stained with H&E to assess lung inflammation. OLYMPUS BX60 was used to acquire the images and analyzed using Scion Image software.

Real-time PCR

mRNA expression levels were determined by using $-\Delta\Delta Ct$ method of real-time PCR as previously described (15, 21) by using primers for *Tnfa* (forward: CCCTCACACTCAGATCATCTTCT, reverse: GCTACGACGTGGGCTACAG), *Il6* (forward: GAGGATACCACTCCCAACAGACC, reverse: AAGTGCATCATCGTTGTTCATACA), *Il1b* (forward: CGCAGCAGCACATCAACAAGAGC, reverse: TGTCCTCATCCTGGAAGGTCCACG), *Opn* (forward: GCCTGTTTGGCATTGCCTCCTC, reverse: CACAGCATTCTGTGGCGCAAGG), *Il10* (forward: GGTTGCCAAGCCTTATCGGA, reverse: ACCTGCTCCACTGCCTTGCT), *Tgfb* (forward: TGGTAACCGGCTGCTGACC, reverse: AGGTGCTGGGCCCTTTCC), *Cxcl1* (forward: TGGGATTCACCTCAAGAACA, reverse: TTTCTGAACCAAGGGAGCTT), *Cxcl2* (forward: CCACCAACCACCAGGCTAC, reverse: GCTTCAGGGTCAAGGGCAAA), *Ccl2* (forward: TCACCTGCTGCTACTCATTCACCA, reverse: TACAGCTTCTTTGGGACACCTGCT), *Ccl3* (forward: TGCTTCTCCTACAGCCGGAAGATT, reverse: TCAGGCATTCAGTTCCAGGTCAGT), *Bacterial 16S ribosomal RNA* (forward: ATTAGATACCCTGGTAGTCCACGCC, reverse:

CGTCATCCCCACCTTCCTCC), *Firmicutes 16S* (forward: ATGTGGTTTAATTCGAAGCA, reverse: AGCTGACGACAACCATGCAC) (22), *Proteobacteria 16S* (Forward: CATGACGTTACCCGCAGAAGAAG, reverse: CTCTACGAGACTCAAGCTTGC) (23), and *Actb* (forward: TGTTACCAACTGGGACGACA, reverse: CTGGGTCATCTTTTCACGGT). *Actb* expression was used as the internal control. Results shown are representatives from multiple independent experiments with similar results. Error bars calculated were based on the calculation of RQ-Min = $2^{-(\Delta\Delta Ct + T * SD(\Delta Ct))}$ and RQ-Max = $2^{-(\Delta\Delta Ct - T * SD(\Delta Ct))}$ from triplicate wells as suggested by a manufacturer of PCR machines (Applied Biosystems). T * SD(Δ*Ct*)) is a square root of x^2+y^2, where x and y are standard deviations of Ct values for a gene of interest and an internal control (β-actin in our case). Error bars for RQ-MIN and RQ-MAX demote acceptable errors for a 95% confidence limit by Student's t test.

Intranasal treatment with antibiotics, NAC and LPS

Mixture of Sulfamethoxazole (0.8 mg/ml) and Trimethoprim (0.16 mg/ml) were used in *in vivo* antibiotics treatment. In intranasal instillation of antibiotics or NAC, 15 μl of antibiotics or NAC solution (50 mM) was administered to a mouse from week 2 to 3 after birth. For intranasal instillation of LPS, 15 μl of LPS (1 ng/ml) was administered daily to a mouse from day 7 to 12 after birth.

Statistical analysis

The two-tailed Student's *t*-test was used for statistical analyses.

Results

Atg7-deficient mice spontaneously develop pulmonary inflammation

We generated *Atg7*$^{fl/fl}$*lysozyme M* (*LysM*)$^{cre/+}$ mice (denoted as "*Atg7* CKO mice" hereafter) and confirmed that *Atg7* mRNA expression and autophagy induction were greatly attenuated in various myeloid cells such as AMs, bone marrow-derived macrophages (BMMs), BM-derived dendritic cells (BMDCs) and neutrophils (PMNs)(Supplementary Fig. 1*A* and *B*). *Atg7* CKO mice appeared healthy with normal reproductive ability. Nevertheless, we noticed that *Atg7* CKO mice showed significantly higher gene expression of pro-inflammatory molecules 7-wk after birth only in the lungs (Fig. 1*A*). To assess more detailed comparison between *Atg7* CKO and *LysM*$^{cre/+}$ (denoted as "WT" hereafter) mice, we examined a time-course of gene expression in the lungs, and found that various pro-inflammatory cytokines (*Tnfa, Il6, Spp1 (Opn)*) and chemokines (*Cxcl1, Cxcl2, Ccl2*) started elevating in the lungs of *Atg7* CKO mice at 3-wk after birth (Fig. 1*B*).

To further evaluate inflammation, we examined the cell infiltration in the lungs. Significantly increased numbers of total cells started to be identified in the lungs of 7-wk old *Atg7* CKO mice (Fig. 2*A*) consistently in every experiment. In particular, more neutrophils ($Ly6G^+CD11b^+$) were identified in the lungs of 3-wk old *Atg7* CKO mice (Fig. 2*B*), reflecting the induction of *Cxcl1* and *Cxcl2* (Fig. 1*B*), neutrophil chemoattractants. By 7-wk old of age, numbers of $Ly6C^+$ macrophages ($Ly6C^+Ly6G^-CD11b^+$), AMs ($CD45^+CD11c^{hi}F4/80^+SiglecF^+$) and cDCs ($CD45^+$ $Ly6G^-$ $CD11c^{hi}$ $F4/80^-$) were also

found significantly higher in the lungs of *Atg7* CKO mice than the WT mice lungs (Fig. 2*B*) (Gating strategy is shown in Supplementary Fig. 1*C–E*). On the other hand, numbers of adoptive immune cells such as $CD4^+$ and $CD8^+$ T cells, B cells, NKT cells were comparable in the lungs of 7-wk old WT and *Atg7* CKO mice (Supplementary Fig. 1*F*, *G*). These results suggested that the pulmonary inflammation in *Atg7* CKO mice is largely mediated by innate immune cells. In accordance to the previous studies reporting GM-CSF-dependent proliferation of AMs (24), expression of *Csf2* mRNA, which encodes GM-CSF, was elevated in the lungs of *Atg7* CKO mice from 3-wk after birth (Fig. 2*C*). Corresponding to the lung-specific upregulation of inflammatory gene expression in *Atg7* CKO mice (Fig. 1*A*), we also confirmed the lung-specific increase in the infiltration of innate immune cells (Fig. 2*D*). However, *Atg7* CKO mice showed normal histology in airway surface areas even in aged mice (7-month)(Supplementary Fig. 2*A*, *B*), suggesting that the spontaneous inflammation in *Atg7* CKO mice was not severe enough to show visible tissue damages. Taken together, the lack of autophagy induces spontaneous pulmonary inflammation characterized by activated expression of proinflammatory genes and myeloid cell infiltration in the lungs.

Littermate comparison between Atg7 CKO and WT mice

Here, environmental factors were ruled out to explain the spontaneous inflammation in *Atg7* CKO mice. To achieve comparison among littermates born from the same parents and raised in the same cage, we bred $Atg7^{fl/fl}LysM^{cre/+}$ mice with $Atg7^{fl/fl}LysM^{+/+}$ and obtained littermates of $Atg7^{fl/fl}LysM^{cre/+}$ (CKO) and $Atg7^{fl/fl}LysM^{+/+}$ (WT), (Fig. 3*A*). Even under the setting, *Atg7* CKO showed elevated *Il6* expression (Fig. 3*B*) and significantly increased innate immune cell infiltration of neutrophils and cDCs in the lungs (Fig. 3*C*).

Atg7-deficient AMs can negatively regulate inflammatory responses

AMs can negatively control pulmonary inflammation. In inflammatory conditions, inhibitory receptors such as CD200R, MARCO and TREM2 are upregulated on the surface of AMs to control pro-inflammatory responses (25–27). In AMs from 7-wk old *Atg7* CKO mice, expression of these receptors was actually higher than that in WT mice (Fig. 4*A*), suggesting that *Atg7*-deficient AMs are well equipped to induce expression of the inhibitory receptors. AMs also suppress inflammation by inducing generation of Tregs (2); thus, we next examine the levels of Tregs in the lungs of 7-wks old *Atg7* CKO mice. Both percentages and absolute numbers of Treg cells were significantly increased in the *Atg7* CKO mice compared to WT mice (Fig. 4*B* and *C*), again indicating no defect in Treg numbers in the lungs of *Atg7* CKO mice. In addition, mRNA expression of *Il10* in the whole lung tissue was elevated in *Atg7* CKO mice in 7-wk old mice (Fig. 4*D*). AMs purified from *Atg7* CKO mice right before the start of pulmonary inflammation at 2-wk of age showed comparative and even higher expression of *Il10* and *Tgfb*, respectively, compared to WT AMs (Fig. 4*E*). Thus, functions to negatively regulate immune responses appeared to be normally functioning in *Atg7*-deficient AMs.

Contribution of environmental microbes in developing spontaneous pulmonary inflammation

Autophagy is known to sequester various microbial pathogens by containing microbes in autophagosomes (4, 9–11). Particularly in pulmonary myeloid cells, including AMs, autophagy plays a critical role in clearing pathogens (5–8). First, we confirmed that lipopolysaccharide (LPS) induces autophagy in AMs from 3-wk old WT mice by identifying LC3 puncta formation (Supplementary Fig. 1*H*). Because it is possible that clearance of environmental pathogens in the lungs was failed due to the absence of autophagy in *Atg7* CKO, burdens of total bacteria were assessed in the lungs by quantitative PCR (qPCR). The burdens were higher in the lungs of *Atg7* CKO mice than those of WT mice 3-wk after birth (Fig. 5*A*), although increase of bacterial burdens were not observed at other time points (2 and 7-wk after birth) and in other organs (spleen, kidney and mLN) (Supplementary Fig. 2*C*). We assessed burdens of *Proteobacteria* and *Firmicutes*, major compositions of lung-resident bacteria in C57BL/6 mice under SPF condition (28), by qPCR using specific primers. Burdens of both bacterial phyla were increased in the lungs of 3-wk old *Atg7*-CKO mice compared to age-matched WT mice (Fig. 5*B*) with increase in burden of *Firmicutes* (3.5 times increase) than that of *Proteobacteria* (1.84 times increase)(Fig. 5*B*). Importantly, the increase of lung bacterial burdens in *Atg7* CKO mice coincides with apparent pulmonary inflammation in the mice around 3-wk after birth (Fig. 1*B*; 2*A*–*C*); thus, it was possible that increased bacterial burdens triggered spontaneous inflammation in the lungs of *Atg7* CKO mice. To evaluate the involvement of bacteria in the development of lung spontaneous inflammation, WT and *Atg7* CKO mice were intranasally instillated with antibiotics every day between the week 2 and 3 after birth. The treatment successfully reduced bacterial burdens (Fig. 5*C*), gene expression of *Il6* and *Cxcl1*, and lung neutrophil counts in *Atg7* CKO mice to similar levels of those in WT mice (Fig. 5*D, E*). Similarly, antibiotics added to drinking water from a prenatal stage to 3-wk after birth also greatly reduced the expression of pro-inflammatory cytokines *Atg7* CKO mice almost to the levels of WT mice (Supplementary Fig. 2*D*–*F*). These results suggested that spontaneous pulmonary inflammation in *Atg7* CKO mice is triggered by, at least in part, environmental bacteria; and the inflammation was preventable with antibiotics.

Activated phenotype of AMs in Atg7 CKO mice

Although cell surface expression of CD11b on AMs from WT mice was not observed, AMs from *Atg7* CKO mice expressed significantly high levels of CD11b (Supplementary Fig. 3*A, B*). Induction of CD11b expression in AMs from *Atg7* CKO mice became apparent at 3-wk after birth (Supplementary Fig. 3*C*), and may be reflecting stimulation of AMs by elevated GM-CSF in the lungs (Fig. 2*C*) as previously reported (29). AMs from 7-wk old *Atg7* CKO mice also showed increased expression levels of CD11c, F4/80 (Supplementary Fig. 3*D*), granularity, and cell sizes (Supplementary Fig. 3*E*), suggesting that *Atg7* CKO AMs were exposed to stimulation. Interestingly, the increase of granularity was observed even in 2-wk old mice, which were yet to show detectable lung inflammation. Thus, it is possible that AMs started to be stimulated as early as 2-wk after birth of *Atg7* CKO mice, then spontaneous pulmonary inflammation manifested at 3-wk after birth. Interestingly, lung-resident DCs in *Atg7* CKO mice showed no difference in CD11c expression, granularity,

and cell size compared to WT mice (Supplementary Fig. 3*F, G*). These results suggested that, compared to lung-resident DCs, AMs are vulnerable and require autophagy to protect them from spontaneous activation.

Autophagy in AMs plays a role in tolerate towards environmental stimuli of low intensity

Our data so far suggested that *Atg7*-deficient AMs over-respond to stimulations at environmental levels. Therefore, we next examined the sensitivity to low levels of LPS in the lungs of *Atg7* CKO mice. Seven-day old WT or *Atg7* CKO mice were intranasally instillated with a low dosage LPS (15 pg/mouse) daily for 5 days, then gene expression was evaluated when the mice were 12-day old (Fig. 6*A*), at which pulmonary inflammation does not occur if naïve (Fig. 1*B*; 2*A, B*). With the LPS treatment, *Atg7* CKO mice increased expression of *Tnfa* and *Il6* mRNA in the lungs, but WT mice did not (Fig. 6*A*). Since the bacterial burdens in the lungs between WT and *Atg7* CKO mice are comparable when they were 2-wk old (Fig. 5*A*), this result suggested that the lack of autophagy lowered the detection threshold of LPS in the lungs. To identify the involvement of AMs in the increased sensitivity of the *Atg7* CKO lungs, AMs from 2-wks old WT and *Atg7* CKO mice were stimulated with 10 ng/ml of LPS *ex vivo*. Indeed, *Atg7*-deficient AMs produced higher levels of TNF-α and CXCL2 than WT AMs, although basal expression levels of the cytokines showed no difference (Fig. 6*B*). Next, we evaluated the LPS sensitivity of *Atg7*-deficient AMs with titrated and low concentrations of LPS *ex vivo*. *Atg7*-deficient AMs turned out to be extremely sensitive to low concentrations (0.3 and 1 ng/ml) of LPS, as shown in the production of TNF-α, while WT AMs were much less sensitive (Fig. 6*C*). Reflecting the sensitivity of *Atg7* CKO AMs, gene expression of proinflammatory cytokines and chemokines were elevated in *Atg7* CKO AMs from 2- and 3-wk old mice (Fig. 6*D*), although the expression levels of PRRs in *Atg7*-deficient AMs was comparable with those in WT AMs (Supplementary Fig. 3*H*). Importantly, in contrast to AMs, BM-derived *Atg7*-deficient macrophages and DCs did not show increased LPS sensitivity, as evaluated by their TNF-α levels (Supplementary Fig. 4*A, B*). Peritoneal-resident macrophages from 2-wk old *Atg7* CKO mice also did not show increased sensitivity in the absence of *Atg7* (Supplementary Fig. 4*C*). These results indicated that the impact of autophagy in LPS sensitivity varies in cell types. Autophagy appears to play a role in tolerating low levels of stimulants in AMs.

Prevention of spontaneous pulmonary inflammation by inhibiting ROS

Autophagy inhibits mtROS production by degrading damaged mitochondria (12). Indeed, *Atg7*-deficient AMs showed increased levels of total and mitochondrial ROS at 2- and 7-wks old compared to WT AMs (Fig. 6*E, F*). Although we do not rule out NADPH oxidase as another source of total ROS, the data suggests that mitochondria is a major source of ROS. Indeed, autophagy is known to sequester damaging mitochondria (30). Interestingly, splenic and peritoneal tissue-resident macrophages obtained from 2-wk old WT and *Atg7* CKO mice showed comparable levels of mtROS production (Supplementary Fig. 4*D*), again suggesting that the impact of autophagy is specific on AMs. Thus, even among tissue-resident macrophages, autophagy-mediated inhibition of mtROS production in a steady state is suggested to be lung-specific. Here, we confirmed *ex vivo* that ROS inhibition with N-acetylcysteine (NAC) attenuated ROS levels in macrophages (Supplementary Fig. 4*E*) and

significantly reduced production of IL-6, TNF-α, CXCL1 and CXCL2 by WT AMs (Fig. 6*G*), and did not alter cell viability in this experiment (Fig. 6*H*). To examine the impact of ROS inhibition *in vivo*, we intranasally instillated NAC to 2-wk old WT and *Atg7* CKO mice for a week (Fig. 6*I*). Without NAC treatment, gene expression of *Il6, Tnfa, Cxcl1*, and *Cxcl2* was greatly higher in *Atg7*-deficient AMs than WT AMs, but NAC treatment successfully narrowed the difference between *Atg7*-deficient AMs and WT AMs (Fig. 6*J*). Importantly, NAC treatment reduced neutrophil recruitment in the lungs of *Atg7* CKO mice, but not of WT mice (Fig. 6*K*). Since a recent study showed that NAC antagonizes proteasome activity (31) and enhances inflammatory responses (32), the possible inhibition of proteasome by NAC in pulmonary inflammation in *Atg7* CKO mice may also be involved. Collectively, these results suggest that autophagy also downregulates mtROS in AMs to further contribute to the inhibition of spontaneous inflammation in an AM-specific manner.

Discussion

Autophagy regulates innate immune responses. For example, autophagy inhibits inflammasome activation by degrading ROS-producing mitochondria and inflammasome assemblies in septic condition (12, 33). On the other hand, autophagy also boosts NFκB-mediated innate immune responses in tissue-resident macrophages and contributes to the host protection against Candida infection as we recently reported (15). Role of autophagy in immune responses has been intensively studied in pathological conditions. However, it has been largely unknown whether and how autophagy is involved in the maintenance of immune homeostasis in non-pathological condition. Here, we found that *Atg7*-deficiency in myeloid cells induces a development of spontaneous pulmonary inflammation due to increased bacterial burdens, enhanced ROS production, and increased sensitivity of AMs during the pre-weaning period. These results indicate that autophagy in pre-mature pups is a part of the lung-specific mechanism to maintain immune ignorance or tolerance not to over-respond to harmless environmental stimuli when pups become adults.

Based on our data, 7-wk old adult mice reduced bacteria to an undetectable level in the lungs both in WT and *Atg7* CKO mice (Fig. 5*A*). The clearance in WT mice may reflect the maturation of the immune system; but, in *Atg7* CKO mice in particular, the clearance may be achieved by the increase of innate immune cells such as neutrophils and monocytes recruited to the lung (Fig. 2*B*). However, when mice were still at 3-wk old, *Atg7* CKO mice had significantly high bacterial burdens (Fig. 5*A*); and this is the time when lung inflammation becomes apparent. Antibiotics treatment prevented spontaneous lung inflammation in *Atg7* CKO mice (Fig. 5*C–E*; Supplementary Fig. 2*D–F*), suggesting the critical involvement of the environmental levels of bacteria in young pups. In addition to the increased bacterial burdens, AMs from *Atg7* CKO mice are sensitive to low levels of LPS stimulation, as shown in Fig. 6*B* and 6*C*. Our data suggested that these two factors predispose the lung of pre-weaned *Atg7* CKO pups to spontaneous inflammation later in their life.

It is of note that our results manifested a clear contrast between the lung and other organs, as well as a contrast between AMs and other macrophages. *Atg7* CKO mice did not show

inflammation in any organs other than the lung at earliest of 7-wk old of age (Fig. 1*A* and 2*D*). Young *Atg7* CKO mice had higher bacterial burdens than WT mice in the lung, but not in other organs (Supplementary Fig. 2*C*). In addition, *Atg7*-deficiency increased mtROS production and sensitivity to TLR4 ligand in AMs (Fig. 6*B–F*), but not in other myeloid cells; such as BMDMs, BMDCs, peritoneal resident macrophages; and splenic macrophages (Supplementary Fig. 4*A–D*). These findings suggest that the lung is a special organ, which takes an advantage of autophagy to maintain its homeostasis, and AMs are most probably attributed to exert the particular function by autophagy. This also reflects the unique setting of the lung with frequent exposures to microbes and dusts in the air, and possibly the distinct biology of AMs evolutionary developed to meet the specific needs for the lung.

In conclusion, *Atg7*-deficiency in myeloid cells makes mice spontaneously develop pulmonary inflammation. Autophagy appeared to protect mice from spontaneous lung inflammation, at least in part, through the following three mechanisms: (1) Maintaining low burdens of environmental microbes in the lung, (2) raising a threshold of AMs in responding to TLR4 stimulation, and (3) keeping mtROS production low in AMs to control inflammation. These mechanisms may mutually influence one another to prevent inflammatory responses. Furthermore, we found that spontaneous pulmonary inflammation in *Atg7* CKO mice can be prevented either by treatment with antibiotics or NAS.

Supplementary Material

Refer to Web version on PubMed Central for supplementary material.

Acknowledgments

We thank Drs. W. Jia, M. He and I. McLeod for their help in setting up the $Atg7^{fl/fl}LysM^{cre/+}$ mouse line and experimental assistance on autophagy. We also thank K. Moore and J. Ashe for their help to maintain $LysM^{cre/+}$ and $Atg7^{fl/fl}LysM^{cre/+}$ mouse lines. This study was supported by NIH R01-AI088100, R21-AI103584 to MLS.

Abbreviation used in this paper

BMMs	bone marrow-derived macrophages
BMDCs	bone marrow-derived dendritic cells
PMN	polymorphonuclear cells
CKO	conditional knock out
AMs	alveolar macrophages
ROS	reactive oxygen species
mtROS	mitochondrial reactive oxygen species
PRRs	pattern recognition receptors
Treg	regulatory T cell
DHE	dihydroethidium
NAC	N-acetyl-L-cyteine

MFI	mean fluorescence intensity
WT	wild type

References

1. Hussell T, Bell TJ. Alveolar macrophages: plasticity in a tissue-specific context. Nature reviews. Immunology. 2014; 14:81–93.
2. Soroosh P, Doherty TA, Duan W, Mehta AK, Choi H, Adams YF, Mikulski Z, Khorram N, Rosenthal P, Broide DH, Croft M. Lung-resident tissue macrophages generate Foxp3+ regulatory T cells and promote airway tolerance. The Journal of experimental medicine. 2013; 210:775–788. [PubMed: 23547101]
3. Gordon SB, Read RC. Macrophage defences against respiratory tract infections. British medical bulletin. 2002; 61:45–61. [PubMed: 11997298]
4. Andrade RM, Wessendarp M, Gubbels MJ, Striepen B, Subauste CS. CD40 induces macrophage anti-Toxoplasma gondii activity by triggering autophagy-dependent fusion of pathogen-containing vacuoles and lysosomes. The Journal of clinical investigation. 2006; 116:2366–2377. [PubMed: 16955139]
5. Yuan K, Huang C, Fox J, Laturnus D, Carlson E, Zhang B, Yin Q, Gao H, Wu M. Autophagy plays an essential role in the clearance of Pseudomonas aeruginosa by alveolar macrophages. Journal of cell science. 2012; 125:507–515. [PubMed: 22302984]
6. Ye Y, Li X, Wang W, Ouedraogo KC, Li Y, Gan C, Tan S, Zhou X, Wu M. Atg7 deficiency impairs host defense against Klebsiella pneumoniae by impacting bacterial clearance, survival and inflammatory responses in mice. American journal of physiology. Lung cellular and molecular physiology. 2014; 307:L355–L363. [PubMed: 24993132]
7. Castillo EF, Dekonenko A, Arko-Mensah J, Mandell MA, Dupont N, Jiang S, Delgado-Vargas M, Timmins GS, Bhattacharya D, Yang H, Hutt J, Lyons CR, Dobos KM, Deretic V. Autophagy protects against active tuberculosis by suppressing bacterial burden and inflammation. Proceedings of the National Academy of Sciences of the United States of America. 2012; 109:E3168–E3176. [PubMed: 23093667]
8. Parihar SP, Guler R, Khutlang R, Lang DM, Hurdayal R, Mhlanga MM, Suzuki H, Marais AD, Brombacher F. Statin therapy reduces the mycobacterium tuberculosis burden in human macrophages and in mice by enhancing autophagy and phagosome maturation. The Journal of infectious diseases. 2014; 209:754–763. [PubMed: 24133190]
9. Orvedahl A, MacPherson S, Sumpter R Jr, Talloczy Z, Zou Z, Levine B. Autophagy protects against Sindbis virus infection of the central nervous system. Cell host & microbe. 2010; 7:115–127. [PubMed: 20159618]
10. Cemma M, Kim PK, Brumell JH. The ubiquitin-binding adaptor proteins p62/SQSTM1 and NDP52 are recruited independently to bacteria-associated microdomains to target Salmonella to the autophagy pathway. Autophagy. 2011; 7:341–345. [PubMed: 21079414]
11. Nicola AM, Albuquerque P, Martinez LR, Dal-Rosso RA, Saylor C, De Jesus M, Nosanchuk JD, Casadevall A. Macrophage autophagy in immunity to Cryptococcus neoformans and Candida albicans. Infection and immunity. 2012; 80:3065–3076. [PubMed: 22710871]
12. Zhou R, Yazdi AS, Menu P, Tschopp J. A role for mitochondria in NLRP3 inflammasome activation. Nature. 2011; 469:221–225. [PubMed: 21124315]
13. Paludan C, Schmid D, Landthaler M, Vockerodt M, Kube D, Tuschl T, Munz C. Endogenous MHC class II processing of a viral nuclear antigen after autophagy. Science. 2005; 307:593–596. [PubMed: 15591165]
14. Cooney R, Baker J, Brain O, Danis B, Pichulik T, Allan P, Ferguson DJ, Campbell BJ, Jewell D, Simmons A. NOD2 stimulation induces autophagy in dendritic cells influencing bacterial handling and antigen presentation. Nature medicine. 2010; 16:90–97.

15. Kanayama M, Inoue M, Danzaki K, Hammer GE, He YW, Shinohara ML. Autophagy enhances NFκB activity in specific tissue macrophages by sequestering A20 to boost early anti-fungal immunity. Nature communications. *In press*.
16. Wen Z, Fan L, Li Y, Zou Z, Scott MJ, Xiao G, Li S, Billiar TR, Wilson MA, Shi X, Fan J. Neutrophils counteract autophagy-mediated anti-inflammatory mechanisms in alveolar macrophage: role in posthemorrhagic shock acute lung inflammation. J Immunol. 2014; 193:4623–4633. [PubMed: 25267975]
17. Aguirre A, Lopez-Alonso I, Gonzalez-Lopez A, Amado-Rodriguez L, Batalla-Solis E, Astudillo A, Blazquez-Prieto J, Fernandez AF, Galvan JA, dos Santos CC, Albaiceta GM. Defective autophagy impairs ATF3 activity and worsens lung injury during endotoxemia. Journal of molecular medicine. 2014; 92:665–676. [PubMed: 24535031]
18. Mayer ML, Blohmke CJ, Falsafi R, Fjell CD, Madera L, Turvey SE, Hancock RE. Rescue of dysfunctional autophagy attenuates hyperinflammatory responses from cystic fibrosis cells. J Immunol. 2013; 190:1227–1238. [PubMed: 23264659]
19. Abdulrahman BA, Khweek AA, Akhter A, Caution K, Kotrange S, Abdelaziz DH, Newland C, Rosales-Reyes R, Kopp B, McCoy K, Montione R, Schlesinger LS, Gavrilin MA, Wewers MD, Valvano MA, Amer AO. Autophagy stimulation by rapamycin suppresses lung inflammation and infection by Burkholderia cenocepacia in a model of cystic fibrosis. Autophagy. 2011; 7:1359–1370. [PubMed: 21997369]
20. Jia W, Pua HH, Li QJ, He YW. Autophagy regulates endoplasmic reticulum homeostasis and calcium mobilization in T lymphocytes. J Immunol. 2011; 186:1564–1574. [PubMed: 21191072]
21. Inoue M, Moriwaki Y, Arikawa T, Chen YH, Oh YJ, Oliver T, Shinohara ML. Cutting edge: critical role of intracellular osteopontin in antifungal innate immune responses. Journal of immunology. 2011; 186:19–23.
22. Guo X, Xia X, Tang R, Zhou J, Zhao H, Wang K. Development of a real-time PCR method for Firmicutes and Bacteroidetes in faeces and its application to quantify intestinal population of obese and lean pigs. Letters in applied microbiology. 2008; 47:367–373. [PubMed: 19146523]
23. Murri M, Leiva I, Gomez-Zumaquero JM, Tinahones FJ, Cardona F, Soriguer F, Queipo-Ortuno MI. Gut microbiota in children with type 1 diabetes differs from that in healthy children: a case-control study. BMC medicine. 2013; 11:46. [PubMed: 23433344]
24. Chen BD, Mueller M, Chou TH. Role of granulocyte/macrophage colony-stimulating factor in the regulation of murine alveolar macrophage proliferation and differentiation. J Immunol. 1988; 141:139–144. [PubMed: 3288696]
25. Gao X, Dong Y, Liu Z, Niu B. Silencing of triggering receptor expressed on myeloid cells-2 enhances the inflammatory responses of alveolar macrophages to lipopolysaccharide. Molecular medicine reports. 2013; 7:921–926. [PubMed: 23314916]
26. Snelgrove RJ, Goulding J, Didierlaurent AM, Lyonga D, Vekaria S, Edwards L, Gwyer E, Sedgwick JD, Barclay AN, Hussell T. A critical function for CD200 in lung immune homeostasis and the severity of influenza infection. Nature immunology. 2008; 9:1074–1083. [PubMed: 18660812]
27. Ghosh S, Gregory D, Smith A, Kobzik L. MARCO regulates early inflammatory responses against influenza: a useful macrophage function with adverse outcome. American journal of respiratory cell and molecular biology. 2011; 45:1036–1044. [PubMed: 21562316]
28. Yun Y, Srinivas G, Kuenzel S, Linnenbrink M, Alnahas S, Bruce KD, Steinhoff U, Baines JF, Schaible UE. Environmentally determined differences in the murine lung microbiota and their relation to alveolar architecture. PloS one. 2014; 9:e113466. [PubMed: 25470730]
29. Kirby AC, Raynes JG, Kaye PM. CD11b regulates recruitment of alveolar macrophages but not pulmonary dendritic cells after pneumococcal challenge. The Journal of infectious diseases. 2006; 193:205–213. [PubMed: 16362884]
30. Nakai A, Yamaguchi O, Takeda T, Higuchi Y, Hikoso S, Taniike M, Omiya S, Mizote I, Matsumura Y, Asahi M, Nishida K, Hori M, Mizushima N, Otsu K. The role of autophagy in cardiomyocytes in the basal state and in response to hemodynamic stress. Nature medicine. 2007; 13:619–624.

31. Halasi M, Wang M, Chavan TS, Gaponenko V, Hay N, Gartel AL. ROS inhibitor N-acetyl-L-cysteine antagonizes the activity of proteasome inhibitors. The Biochemical journal. 2013; 454:201–208. [PubMed: 23772801]

32. Qureshi N, Morrison DC, Reis J. Proteasome protease mediated regulation of cytokine induction and inflammation. Biochimica et biophysica acta. 2012; 1823:2087–2093. [PubMed: 22728331]

33. Nakahira K, Haspel JA, Rathinam VA, Lee SJ, Dolinay T, Lam HC, Englert JA, Rabinovitch M, Cernadas M, Kim HP, Fitzgerald KA, Ryter SW, Choi AM. Autophagy proteins regulate innate immune responses by inhibiting the release of mitochondrial DNA mediated by the NALP3 inflammasome. Nature immunology. 2011; 12:222–230. [PubMed: 21151103]

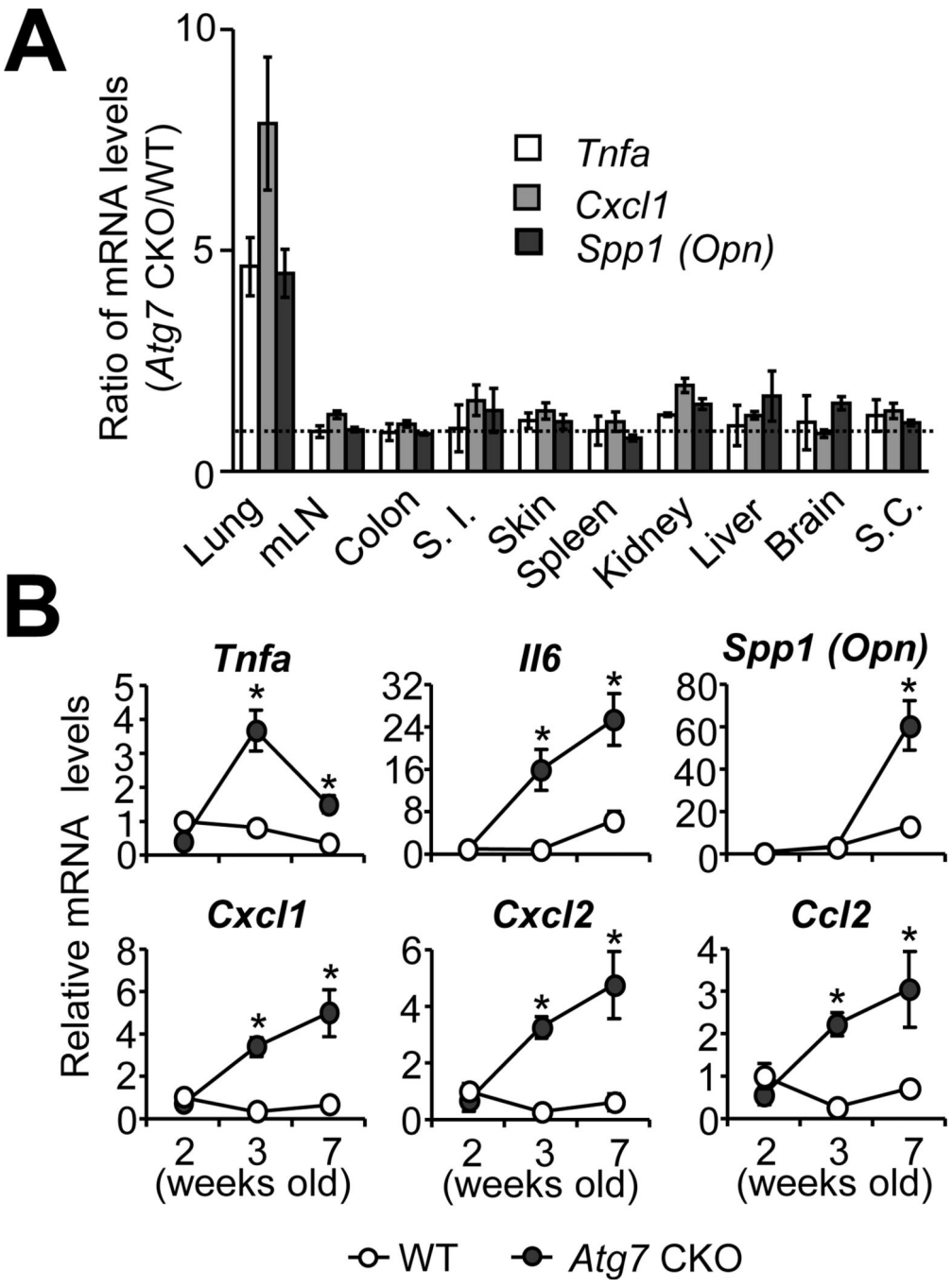

FIGURE 1. Elevated expression levels of cytokines and chemokines in the lung of *Atg7* CKO mice

A, Gene expression of *Tnfa, Cxcl1 and Spp1 (Opn)* in various tissues obtained from 7-wk old WT and *Atg7* CKO mice. Shown are values of gene expression levels in *Atg7* CKO (*n=4*) mice relative to those in WT mice (*n=3*). *B*, Gene expression in the lung of WT and *Atg7* CKO mice evaluated by qPCR. Data are representative of two independent experiments. Error bars represent mean ± SD. *; $p<0.05$.

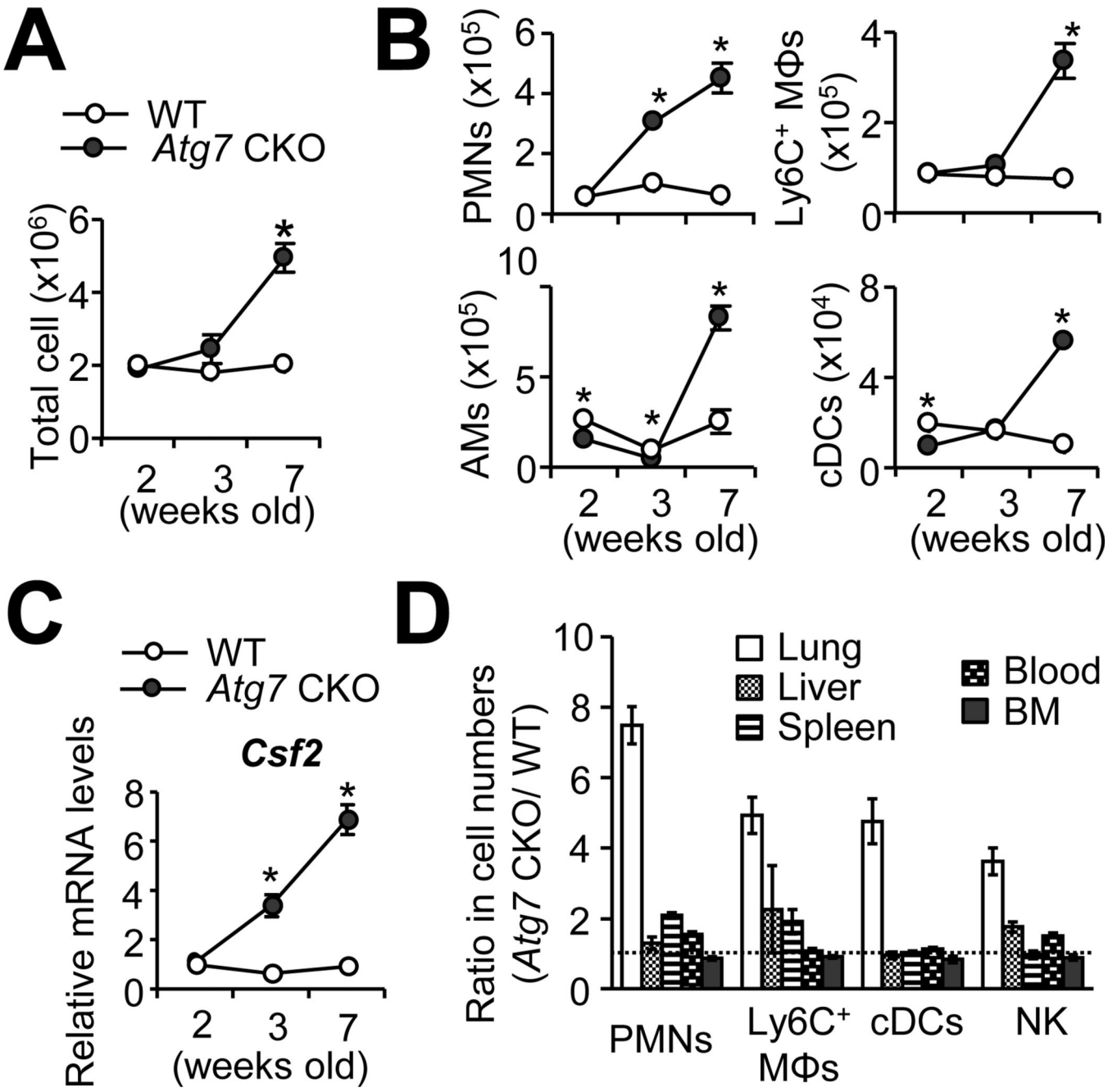

FIGURE 2. Increased cell infiltration in the lung of *Atg7* CKO mice

A, Total cell numbers in the lung of WT and *Atg7* CKO mice at the indicated ages. *B*, Numbers of innate immune cells in the lung of WT and *Atg7* CKO mice. Percentages of neutrophils (Polymorphonuclear leukocytes, PMNs; $CD11b^{+}Ly6G^{+}$), $Ly6C^{+}$ macrophages ($Ly6C^{+}$ MΦ; $CD11b^{+}Ly6C^{+}CD11c^{-}$), AMs ($CD11c^{hi}F4/80^{+}$Siglec F^{+}) and cDCs ($CD11c^{hi}F4/80^{-}$) were analyzed by flow cytometry. *C*, *Csf2* gene expression in the whole lung. Levels of mRNA expression were detected by qPCR. *D*, Cellularity in various tissues of 7-wk old WT and *Atg7* CKO mice. Shown are values of gene expression levels in *Atg7*

CKO (*n=4*) mice relative to those in WT mice (*n=3*). Data are representative of at least two independent experiments. Error bars represent mean ± SD. *; $p<0.05$.

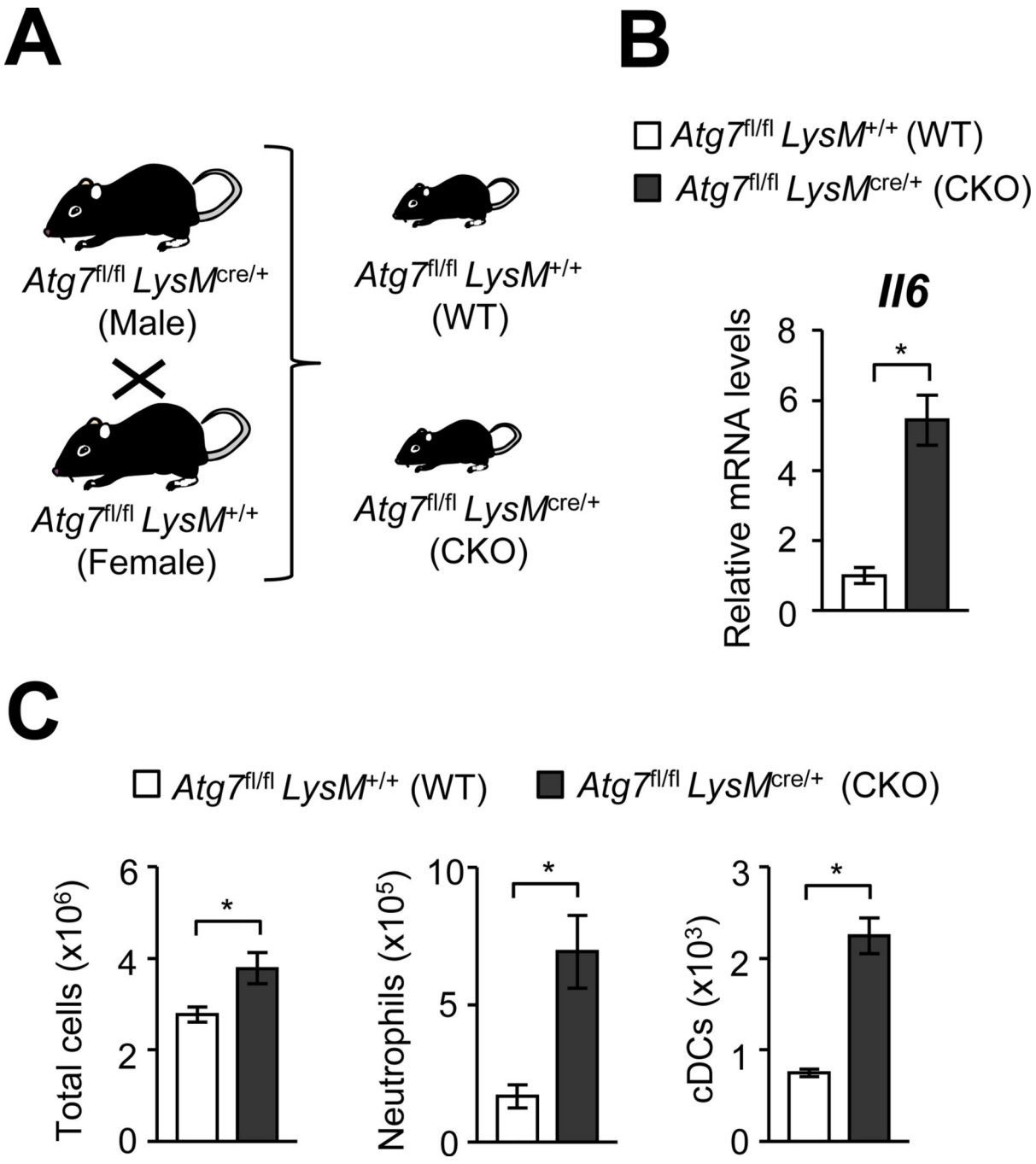

FIGURE 3. *Atg7* CKO mice still show pulmonary inflammation regardless of housing environment

A, *Atg7*$^{fl/fl}$*LysM*$^{cre/+}$ (*Atg7* CKO) and *Atg7*$^{fl/fl}$*LysM*$^{+/+}$ (Atg7 WT) mice were mated to obtain littermates of *Atg7* CKO and Atg7 WT genoptypes. *B*, Expression of *Il6* in whole lung tissues obtained from 7-wk old *Atg7* CKO and WT mice. Error bars denote RQ-Max/Min as described in the Method section. *C*, Cellularity in the lung of *Atg7* CKO and WT mice. *n=3* per group. Error bars represent mean ± SD. Data are representative of two independent experiments. *; $p<0.05$.

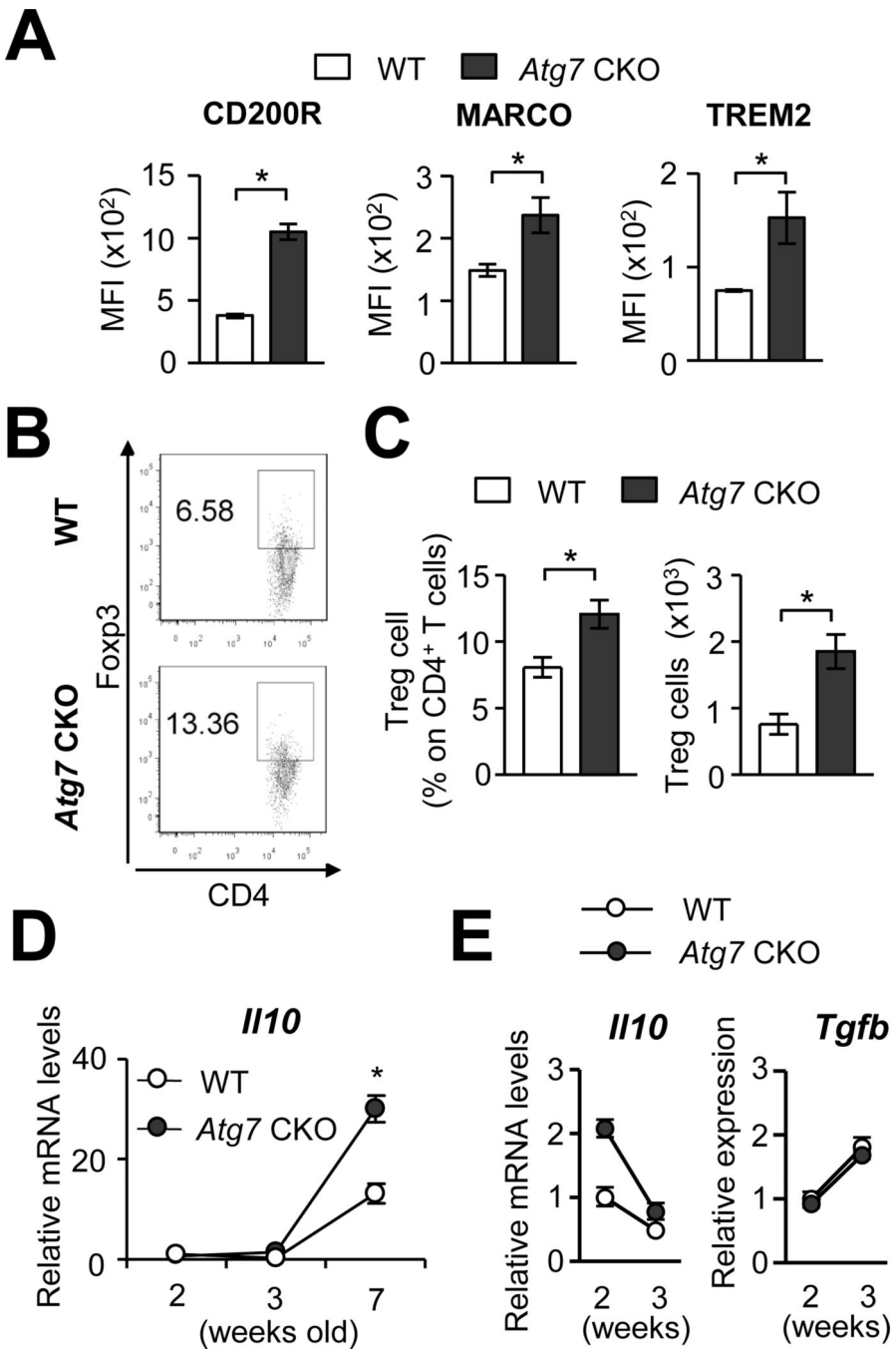

FIGURE 4. Anti-inflammatory responses in the lung of *Atg7* CKO mice

A, Expression levels of CD200R, MARCO and TREM2 on the surface of AMs obtained from 7-wk old *Atg7* CKO and WT mice. *B*, Representative flow cytometry results of Foxp3$^+$ regulatory T cells in the lung of 7-wk old *Atg7* CKO and WT mice. *C*, Frequency and total numbers of Foxp3$^+$ regulatory T cells in the lung of 7-wk old *Atg7* CKO and WT mice. *D*, *Il10* mRNA expression in lung tissues obtained from *Atg7* CKO (*n=4*) and WT (*n=3*) mice. *E*, Levels of *Il10* and *Tgfb mRNA* in AMs obtained from 2- or 3-wk old *Atg7* CKO and WT mice. Each sample was pooled form 3 mice. Error bars in A–C represent mean ± SD. Error

bars in D and E denote RQ-Max/Min as described in the Method section. Data are representative of two independent experiments. *; $p<0.05$.

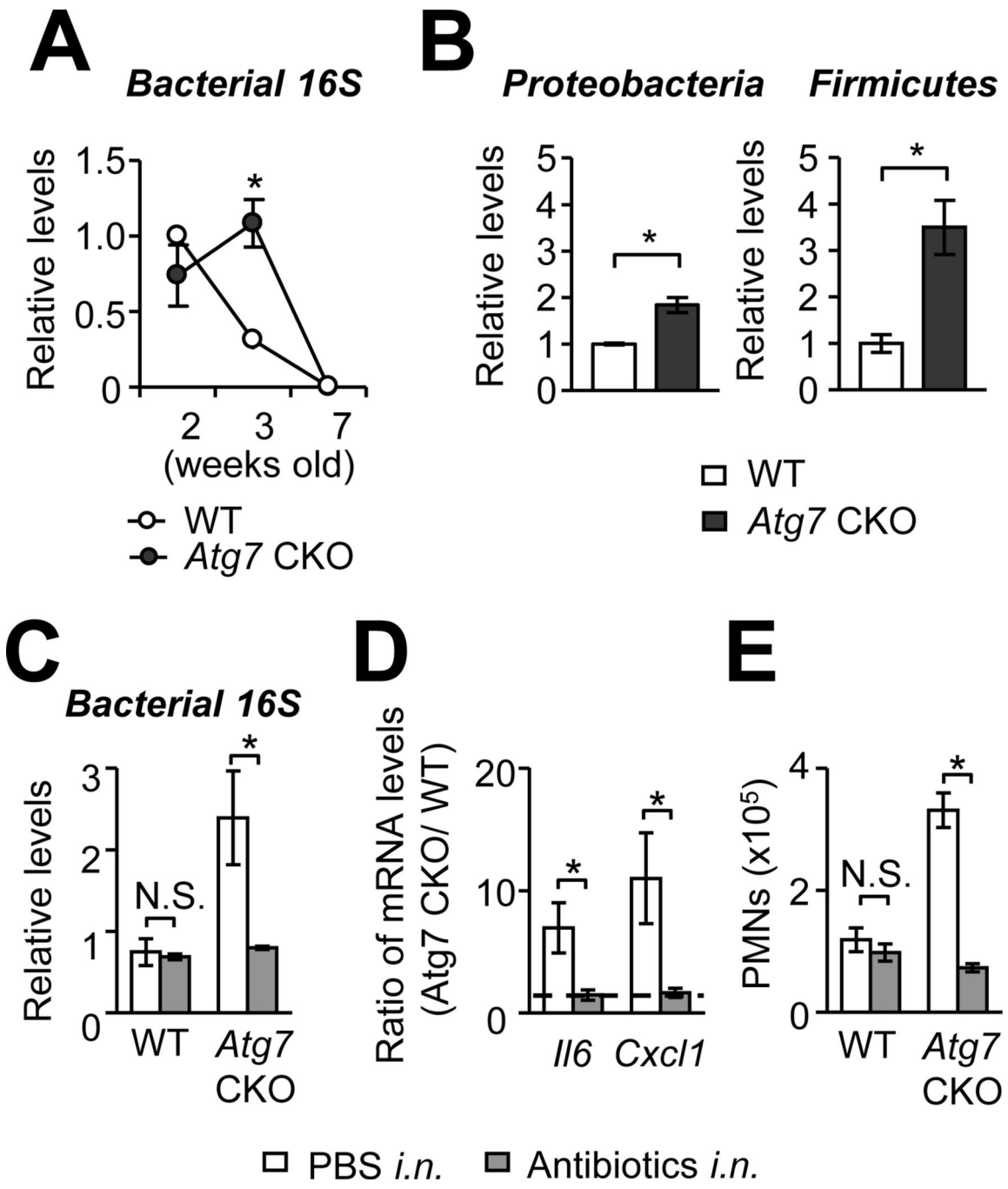

FIGURE 5. ***Atg7*-deficiency increases bacterial burdens in the lung**

A and *B*, Bacterial burdens in the lung of WT and *Atg7* CKO mice. Burdens of total bacteria (A), *Proteobacteria* and *Firmicutes* (B) were evaluated by qPCR by using universal bacterial 16S rRNA primers and phylum-specific 16S rRNA primers, respectively (normalized to mouse *Actb*). *C*, Bacterial burdens in antibiotics-treated WT and *Atg7* CKO mice. Mice were intranasally instillated with antibiotics daily from 2 to 3 wk after birth. mRNA were isolated from the whole lung, and bacterial burdens were evaluated by qPCR. *D*, Comparison of expression levels of *Il6* and *Cxcl1* in the lung between WT and *Atg7* CKO

mice with or without antibiotics treatment. Shown are values of gene expression in *Atg7* CKO mice relative to that in WT mice. *E*, Numbers of neutrophils (PMNs) in the lung of WT and *Atg7* CKO mice with or without antibiotics treatment. $n=3$ per group. Data are representative of at least two independent experiments. Error bars represent mean ± SD. *; $p<0.05$.

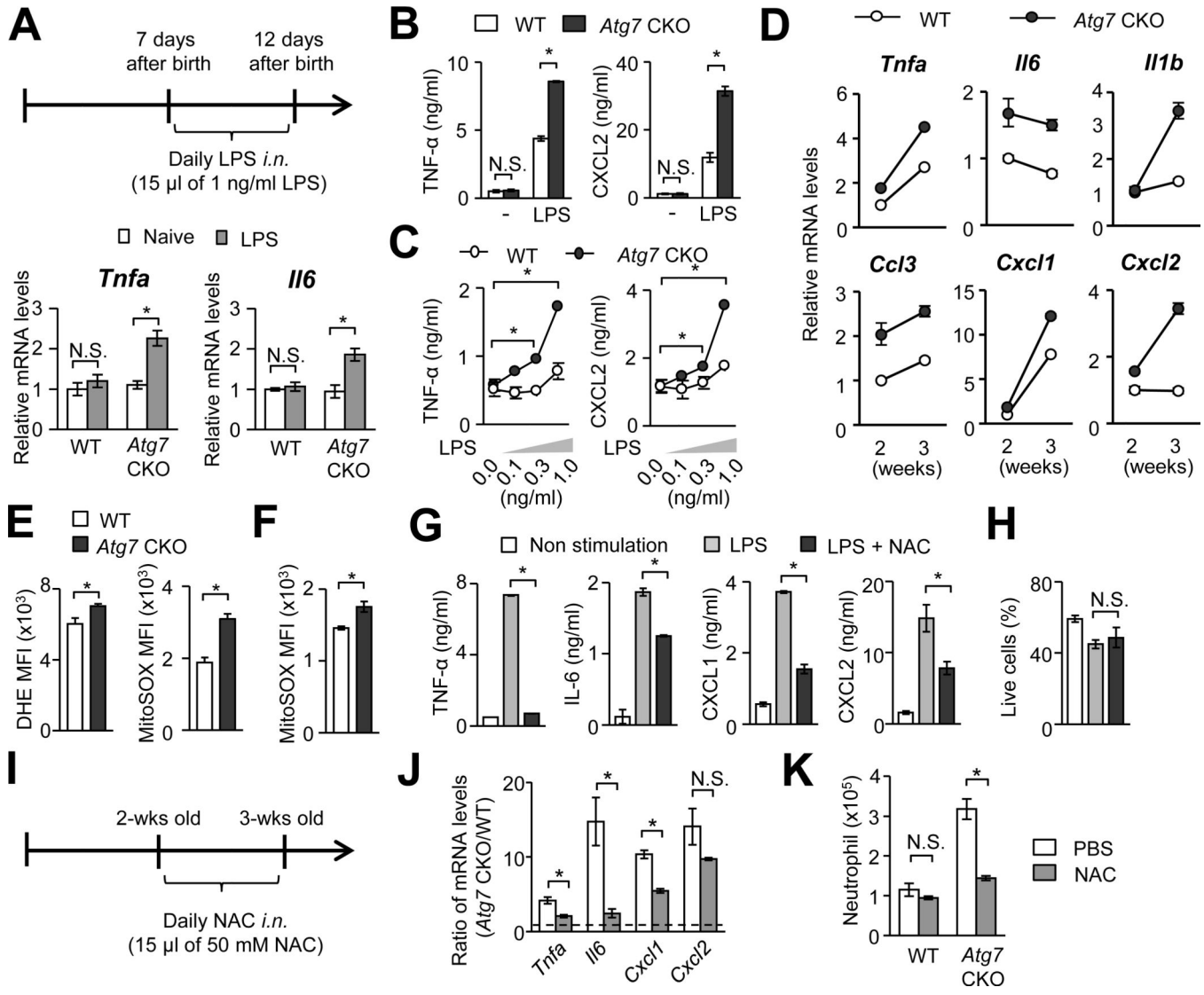

FIGURE 6. *Atg7*-deficiency enhances sensitivity of AMs to low level stimulations

A, Intranasal instillation of LPS (15 pg/mouse) induced expression of *Il6* and *Tnfa* mRNA in the lung of 2-wk old *Atg7* CKO mice, but not WT mice. *n=3* per group. *B* and *C*, AMs, obtained from 2-wk old WT and *Atg7* CKO mice, were cultured (2.5×10^5/ml) with 10 ng/ml (B) or 0.1–1 ng/ml (C) of LPS for 24 hrs. Levels of TNF-α and CXCL2 in culture supernatants were evaluated. *n=3*. *D*, Gene expression of cytokines and chemokines in the AMs isolated from 2 and 3-wk old WT and *Atg7* CKO naïve mice. Error bars denote RQ-Max/Min as described in the Method section. Each sample was pooled form 3 mice. Error bars in D and E denote RQ-Max/Min. *E* and *F*, ROS production in AMs from 7-wk (E) and 2-wk old (F) WT and *Atg7* CKO naïve mice. Production of total and mtROS was evaluated by DHE and MitoSOX, respectively. *n=3* per group. *G*, Comparison of cytokine and chemokine production in WT AMs under ROS inhibition. AMs (2.5×10^5/ml) isolated from 2-wk old WT mice were stimulated with LPS (10 ng/ml) in the presence or absence of NAC (10 mM) for 24 hrs. Cytokine and chemokine production in culture supernatants were evaluated by ELISA. *H*. Proportions of live cells at the time of supernatant harvest in (G).

n=3 per group. *I–K*, Experimental scheme of intranasal instillation of NAC (I). WT and *Atg7* CKO mice were intranasally treated with 15 μl of 50 mM NAC daily for 7 days starting from 2-wk after birth. Lungs were harvested at the completion of NAC treatment. Shown are levels of indicated mRNA as expression ratios between *Atg7*-deficient AMs and WT AMs (J), and numbers of neutrophils in the lung (K). *n=3–4* per group. Data are representative of at least two independent experiments. Error bars represent mean ± SD. *; $p<0.05$.